Electrochemical Characterizations of Nickel Deposition on Aromatic Dithiol Monolayers on Gold Electrodes

Hiroyuki Noda,*,†,§ Yian Tai,‡ Andrei Shaporenko,‡ Michael Grunze,‡ and Michael Zharnikov*,‡

Division of Chemistry, Graduate School of Science, Hokkaido University, Kita-ku, Sapporo 060-0810, Japan, and Angewandte Physikalische Chemie, Universität Heidelberg, Im Neuenheimer Feld 253, 69120 Heidelberg, Germany

Received: April 27, 2005; In Final Form: September 2, 2005

The electronic properties of pristine and cross-linked (CL) self-assembled monolayers (SAMs) of [1,1′;4′,1″-terphenyl]-4,4″-dimethanethiol (TPDMT) on Au were studied by electrochemical measurements, including cyclic voltammetry and impedance spectroscopy. In addition, nickel deposition onto the TPDMT and CL-TPDMT substrates was investigated. In all cases, the TPDMT and CL-TPDMT films were found to be insulators, which effectively blocked the ionic permeation of electrolyte, preventing direct access of ions to the Au electrode. At the same time, CL-TPDMT is a better electric insulator than the pristine TPDMT SAM. The top Ni layer in the Ni/CL-TPDMT/Au arrangement was electrically isolated from the Au substrate, and no short circuits occurred. This layer was found to be conductive and relatively stable in the broad potential range in the electrolyte solution.

1. Introduction

Thin organic films have received a great deal of attention in recent years as molecular electronics assemblies and components of nanoscale devices. In particular, self-assembled monolayers (SAMs), which are well-ordered and densely packed organic films composed of chemisorbed rodlike molecules,[1−3] have the potential to be used as ultrathin insulating layers in novel electronic and spintronic devices.[4−7]

For the practical implementation of this idea, it is quite important to understand the electronic conductivity across a SAM sandwiched between two metal electrodes. This can be done using e.g. a conducting atomic force microscopy (AFM)[8] or a mercury-drop method.[9] Using these approaches, the electronic conductivity across nanometer-thick organic film between two metal electrodes has been first investigated for aliphatic systems, including fatty acids,[10] *n*-alkyltrichlorosilanes,[11,12] and *n*-alkylthiols.[13] All these films were found to be good electronic insulators. In particular, *n*-alkyltrichlorosilanes immobilized between SiO_2 and Al surfaces (a semiconductor/insulator/metal structure) exhibited very low conductivity.[11,12] Similar conductivity was reported for $Hg-S(CH_2)_{n>10}CH_3/CH_3-(CH_2)_{n>10}S-Hg$ arrangements (mercury-drop method).[13] Later, the electronic properties of the aromatic SAMs in the metal−SAM−metal assembly were also studied.[9,14] It was found that the corresponding SAMs are insulating as well, even though they exhibit a slightly better conductivity as compared to the aliphatic systems. [9,14]

Recently, we have investigated a SAM of [1,1′:4′,1″-terphenyl]-4,4″-dimethanethiols [$HS-CH_2-(C_6H_4)_3-CH_2-SH$, TPDMT] on polycrystalline Au(111) substrate[15] and found that these films exhibit high orientational order and dense packing on Au(111),[15] similar to the SAMs of biphenyl-substituted or 4,4′-terphenyl-substituted alkanethiols, $CH_3-(C_6H_4)_2-(CH_2)_n-SH$ and $C_6H_5-(C_6H_4)_2-(CH_2)_n-SH$, respectively, at odd *n*.[16−20] Furthermore, using Ni as a test metal adsorbate, we demonstrated that the stable metal overlayer could be fabricated at the SAM−ambient interface of the TPDMT film, if it is cross-linked prior to the deposition, which can be achieved by electron irradiation.[21,22]

In this study, we investigated the electronic properties of the TPDMT SAM and Ni deposition onto the TPDMT substrate by using electrochemical tools, including cyclic voltammetry and impedance spectroscopy. The effect of cross-linking (CL) on electric properties of the TPDMT SAM was also monitored. In particular, we were interested in the electrochemical blocking properties of the TPDMT and CL-TPDMT monolayers against the permeation of ions and in the electrochemical stability of these films and the Ni/CL-TPDMT bilayer in an aqueous electrolyte solution.

2. Experimental Setup

The synthesis of the TPDMT and terphenyl-4-methanthiol (TPMT—it has been used as a reference in some of the experiments) compounds has been described elsewhere (see refs 15 and 19, respectfully). The gold substrates were prepared by thermal evaporation of 100 nm of Au (99.99% purity) onto polished single-crystal silicon (100) wafers (Silicon Sense), which had been precoated with a 5 nm titanium adhesion layer. The resulting gold films are polycrystalline, with a grain size of 20−50 nm. The grains predominantly exhibit an (111) orientation. The SAMs were formed by immersion of freshly prepared substrates into a 1 mM TPDMT solution in tetrahy-

* Corresponding author. Telepone: (H.N.) +81-22-795 5869; (M.Z.) +49-6221-54 4921. Fax: (H.N.) +81-22-795-5869; (M.Z.) +49-6221-54 6199). E-mail: (H.N.) hirond@atom.che.tohoku.ac.jp; (M.Z.) Michael.Zharnikov@urz.uni-heidelberg.de.

† Hokkaido University.

§ Present address: Department of Applied Chemistry, Graduate School of Engineering, Tohoku University, Aoba-yama 6-6-04, Sendai 980-8579, Japan.

‡ Universität Heidelberg.

10.1021/jp052180a CCC: $30.25
Published on Web 11/01/2005

drofuran (Sigma-Aldrich), which was stabilized with 0.1% hydroquinone (Merck), at room temperature for 24 h. After immersion, the samples were carefully rinsed with pure solvent and blown dry with argon. No evidence for impurities or oxidative degradation products was found by X-ray photoelectron spectroscopy and infrared spectroscopy.

Some of the fabricated TPDMT films were irradiated by electrons with a kinetic energy of 10 eV to achieve an extensive cross-linking of the aromatic backbones within the film.[23,24] The dose was 40−45 mC/cm^2. For the irradiation, a current density of ≈2.5 μA/cm^2 was used; electon exposure was calibrated with a Faraday cup.

Pristine and cross-linked TPDMT films served as substrates for Ni evaporation. Ni (Goodfellow, 99.999% purity) was evaporated from a commercial e-beam evaporator (Omicron) with a deposition rate of 0.2 nm/min; the rate was calibrated by a commercial quartz crystal microbalance sensor (Inficon). The evaporation was performed at a base pressure better than 1.5×10^{-9} Torr; the substrates were kept at room temperature. The Ni coverage was 5−6 monolayers; it was estimated relative to the Au(111) surface. For the electrochemical measurements, the samples were taken from the evaporation chamber, exposed to ambient, and put into an electrochemical solution. Transfer of the sample was presumably accompanied by a partial oxidation of the Ni film.

Electrochemical measurements on the TPDMT SAMs and Ni−TPDMT bilayers were carried out with a ZAHNER IM6e impedance measurement unit (ZAHNER Elektrik) under an argon gas atmosphere and at room temperature. Both cyclic voltammetry and impedance spectroscopy experiments were performed. Ag/AgCl and Pt mesh electrodes were used as the reference and counter electrodes, respectively. The area of the SAM samples used as the working electrode was varied, but we tried to keep it close to 1 cm^2. The bare Ni electrode, used in some experiments as a reference, was a Ni rod purchased from Goodfellow. An aqueous (Milli-Q water, 18 MΩ) solution of 0.1 M Na_2SO_4 (analytical grade, ACROS ORGANICS) or $HClO_4$ (analytical grade, ACROS) was used as an electrolyte. Prior to the electrochemical measurements, the electrolyte solution was deaerated by bubbling argon gas for 15 min. Cyclic voltammograms were acquired with a constant scan rate of 0.1 V s^{-1} in the potential range between −0.5 and 0.6 V. Impedance spectra were recorded between 100 kHz and 50 MHz under sinusoidal potentials with an amplitude of 10 mV. To estimate the electrochemical parameters from the experimental data, their theoretical analysis was performed. The whole system was approximated by a simplified equivalent circuit model composed of serial resistance R_s, interface capacitance C, and interface resistance R_p.[25] The estimated error of the data analysis was ±10%.

3. Results and Discussion

3.1. Cyclic Voltammetry. In this section, we will discuss the electrochemical behavior of the TPDMT SAMs and Ni−TPDMT systems as a function of electrode potential. This will elucidate the blocking properties of these monolayers against permeation of ions and establish the potential range of electrochemical stability.

Figure 1 shows cyclic voltammograms (CVs) of the bare Au, TPDMT/Au, CL-TPDMT/Au, Ni/TPDMT/Au, and Ni/CL-TPDMT/Au in a double-layer potential range. The CVs were obtained in the absence of the redox-active species of dilute Na_2SO_4. As compared to the bare gold electrode (Figure 1a), all SAM- and Ni−SAM-covered Au electrodes (Figure 1b−e)

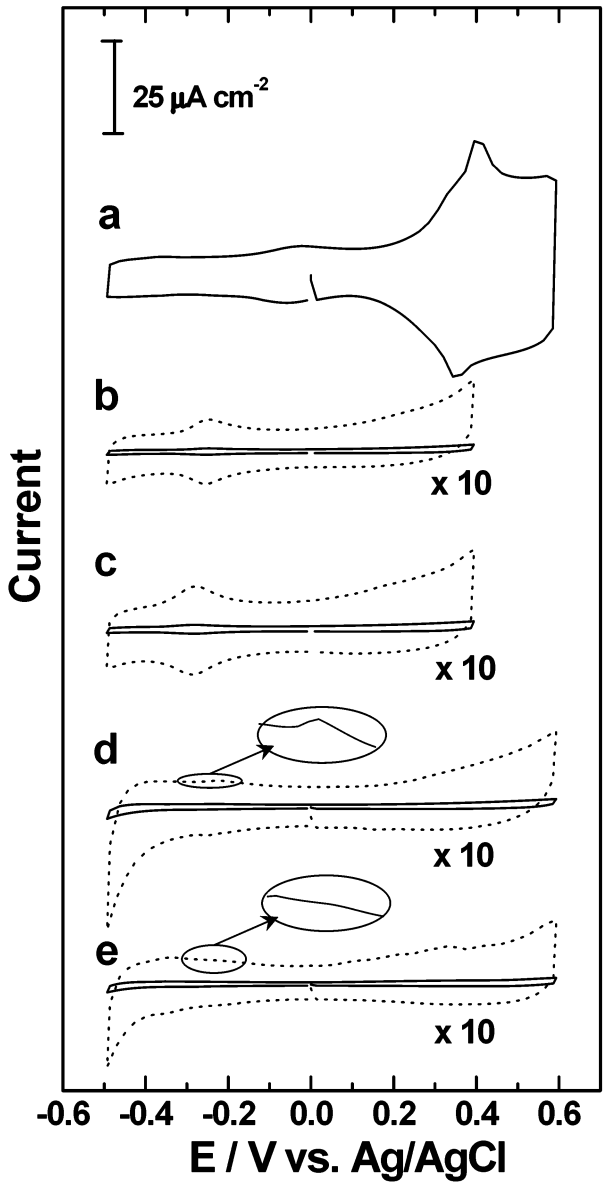

Figure 1. Cyclic voltmmograms (CV) of bare and SAM-covered gold electrodes in 0.1 M Na_2SO_4: (a) bare, (b) TPDMT, (c) CL-TPDMT, (d) Ni/TPDMT, and (e) Ni/CL-TPDMT. Dotted curves represent the CVs scaled up by a factor of 10. The scan rate was 0.1 V s^{-1}.

exhibit markedly reduced double-layer charging currents and an almost potential-independent behavior, which is characteristic for thin layers having a low dielectric constant and blocking ion transfer to the electrode.[26−28] For the pristine TPDMT SAM (Figure 1b), this result implies that this film is well-organized and densely packed, which agrees with previous results.[15,29] In addition, it is electrochemically stable in an aqueous electrolyte solution. Another implication is that the ion blocking behavior of the TPDMT films is affected neither by cross-linking nor by Ni evaporation.

When the current range of the CVs in Figure 1 was enlarged (dotted lines), the shape of these curves was found to be slightly different for the different systems. For both pristine TPDMT and CL-TPDMT covered gold electrodes, a small reversible peak was observed at around −0.28 V, although there was no redox-active species in the solution. The shape of this peak was independent of the scan rate, when it was varied in a range of 50−1000 mV s^{-1}. It might be possible to assign the redox peak to a reaction of the terminal thiol group; however, the same

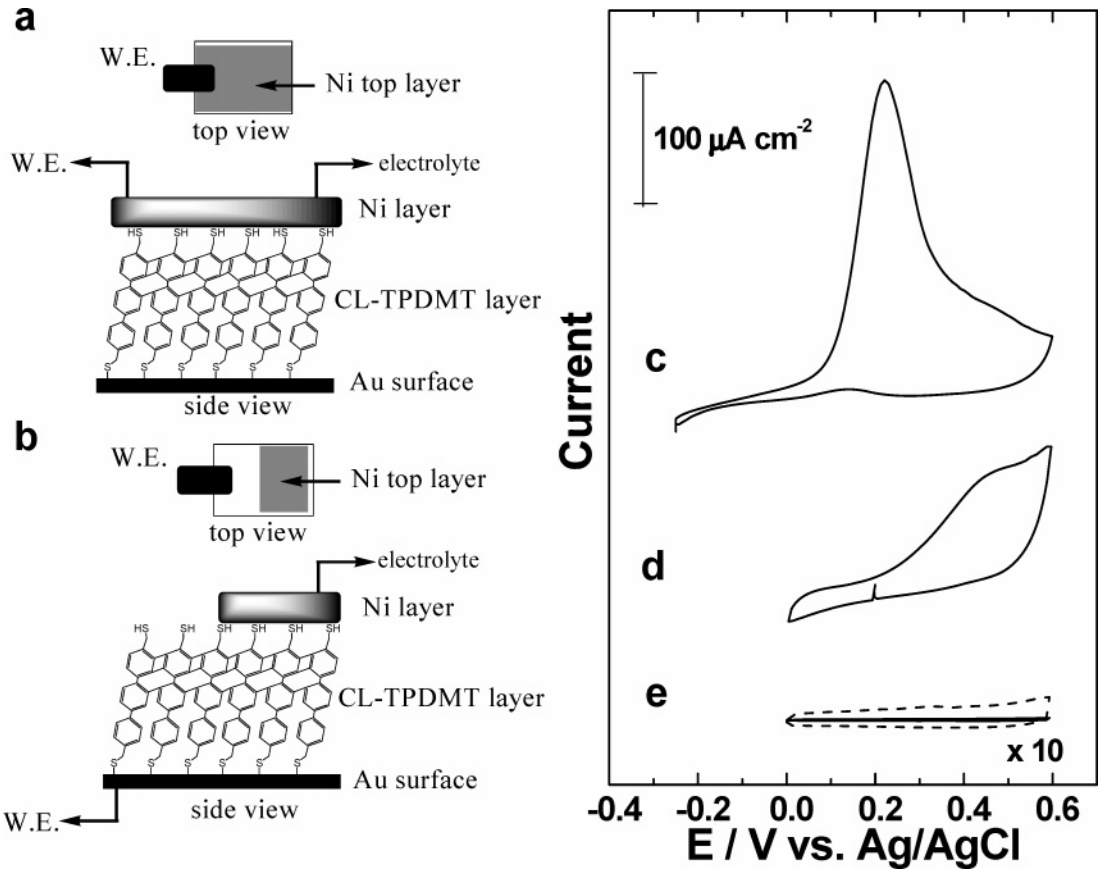

Figure 2. Schematic representations of two different experimental arrangements and the respective cyclic voltammograms (CV) for Ni/CL-TPDMT/Au in 0.1 M $HClO_4$. In a and d, the top Ni layer was contacted by the working electrode. In b and e, the Au substrate was contacted. For comparison, the cyclic voltammogram of a bare Ni electrode is presented in c. The dotted curve in e represents the respective CV scaled up by a factor of 10. The scan rate was 0.1 V s^{-1}.

behavior was observed for the TPMT SAM on Au (the results are not shown here), which does not have such a terminal moiety. Weighting different possibilities, we tentatively assign this peak to a reaction involving the internal phenyl rings in the aromatic backbone of the TPDMT molecules.

In contrast to TPDMT/Au and CL-TPDMT/Au, there were no such noticeable redox peaks for the Ni/TPDMT/Au and Ni/CL-TPDMT/Au samples. There was still a very weak feature in the case of the Ni/TPDMT/Au system (see the CV enlargement presented in the inset of Figure 1d), for which most of the Ni adsorbate penetrates into the TPDMT film and diffuses to the TPDMT/Au interface.[21,22] At the same time, the redox peak disappeared completely (see the CV enlargement presented in the inset of Figure 1e) in the case of the Ni/CL-TPDMT/Au system, for which no penetration of Ni into the CL-TPDMT film was observed, so that a Ni overlayer was formed at the CL-TPDMT−ambient interface.[21,22] Considering the disappearance of the redox peak, we assume that the Ni overlayer covered the CL-TPDMT SAM completely, preventing the access of ions, which are the electron source of a redox reaction, into the interior of the CL-TPDMT film.

The important point to note is that the Ni overlayer is relatively stable within the broad potential range in the electrolyte solution. Generally, in the case of bare Ni electrode, the dissolving reaction of Ni occurs in an acidic solution at −0.25 V vs NHE (or around 0 V vs Ag/AgCl),[30] which was exactly reproduced by us for this particular sample, as shown in Figure 2c, in which the respective CV is presented. Accordingly, at the beginning of our experiments, we considered the possibility that the Ni overlayer in the Ni/CL-TPDMT/Au arrangement will dissolve to the solution phase under similar electrochemical conditions. To monitor the respective processes, two different Ni/CL-TPDMT/Au samples were prepared as schematically shown in Figure 2a,b: either the top Ni layer (Figure 2a) or Au substrate (Figure 2b) were contacted by the working electrode outside of the electrolytic solution. In the case of the Ni top layer contact, a large current similar to that for the bare Ni electrode was observed at +0.4 V, as shown in Figure 2d. This finding suggests that the top Ni layer is conductive (despite a partial oxidation due to the exposure to ambient and the immersion into the electrolyte solution) and that electron-transfer reaction occurs directly through this layer to the electrolyte solution. At the same time, no large current was observed in the potential region between 0 and 0.6 V in the case of the substrate contact as shown in Figure 2e, which implies that the dissolving reaction of Ni did not occur for this particular electrode arrangement. Furthermore, the shape of the respective CV was different from that of the pristine TPDMT SAM (Figure 1b), while identical shapes would be expected, if all Ni atoms were removed from the SAM−ambient interface. Therefore, we believe that the dissolving reaction of Ni did not occur in the case of the Ni/TPDMT/Au arrangement under the given electrochemical conditions. The reason for this special behavior is presumably the electric insulation of the Ni overlayer from the gold electrode by the CL-TPDMT film, so that the potentials on the former overlayer and the latter electrode were quite different.

To get a deeper insight into the insulator properties of the CL-TPDMT film, we have measured CV of CL-TPDMT/Au in the presence of redox-active species in the solution and

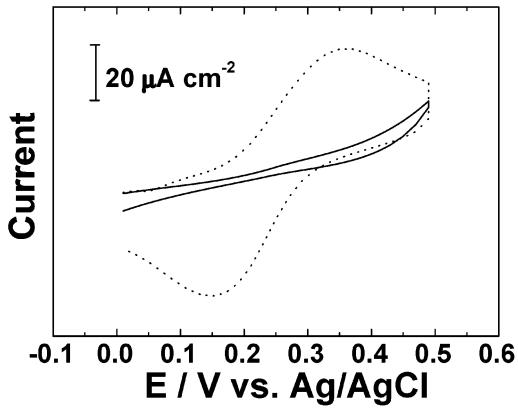

Figure 3. Comparison of the cyclic voltammograms of $Fe(CN)_6^{3-/4-}$ for a bare (dotted line) and CL-TPDMT-coated (solid line) gold electrode in 0.1 M Na_2SO_4.

compared it with the respective curve for the bare gold electrode. In the presence of 1 mM of a redox couple, $Fe(CN)_6^{3-}$/$Fe(CN)_6^{4-}$ the voltammogram of the bare gold electrode exhibited the typical shape for diffusion-limited electron-transfer processes, as shown in Figure 3 (dashed line) in which the respective curve is presented. In contrast, after the gold electrode was coated with the CL-TPDMT film, the global shape of the voltammogram trace (solid line in Figure 3) was significantly changed. This change in the current response suggests a highly effective coverage of the electrode surface by the CL-TPDMT film with no or very few defects that can serve as a transfer channel for the redox species or active sites for electrochemistry.

3.2. Impedance Spectroscopy. Electrochemical impedance measurements based on the response of an electrochemical cell to a small-amplitude alternating signal offer a convenient method to study electronic properties of our systems.[30] Figure 4 shows a series of electrochemical impedance spectra of TPDMT/Au, CL-TPDMT/Au, Ni/TPDMT/Au, and Ni/CL-TPDMT/Au in 0.1 M Na_2SO_4. From the cyclic voltammogram measurements, we choose the bias potential across the interface as 0.0 V, looking for the smallest charge current potential to minimize electrochemical reactions at the interface.

As the reference, the impedance spectrum of the bare gold electrode was measured and the respective electrochemical parameters were calculated, assuming a double-layer formation at the gold electrode/electrolyte interface and the ohmic behavior of the electrolyte solution and the contacts in the high-frequency regime. Within this standard model, we obtained a serial resistance (R_s) of 12.04 Ω and a double-layer capacitance (C_{dl}) of 14.26×10^{-6} F cm^{-2}.

To analyze the impedance of the TPDMT-modified Au electrode, we fitted the respective experimental impedance spectra by theoretical curves, which were calculated using a simplified equivalent circuit model composed of serial resistance R_s, interfacial capacitance C, and interface resistance R_p as shown in the inset of Figure 4a.[25] The derived values of these parameters for all investigated systems are summarized in Table 1. According to this table, the capacitance values for the pristine TPDMT SAMs are very similar to previously reported values for *p*-terphenyl mercaptan SAM on Au.[26]

Although the value of capacitance was almost the same for all systems of this study, there was a difference in the value of interfacial resistance between the pristine and cross-linked TPDMT SAMs. The observed trend is an increase of the resistance upon the cross-linking. This result indicates that the CL-TPDMT film possesses better insulating properties than the pristine TPDMT SAM. This may be related to a decreasing

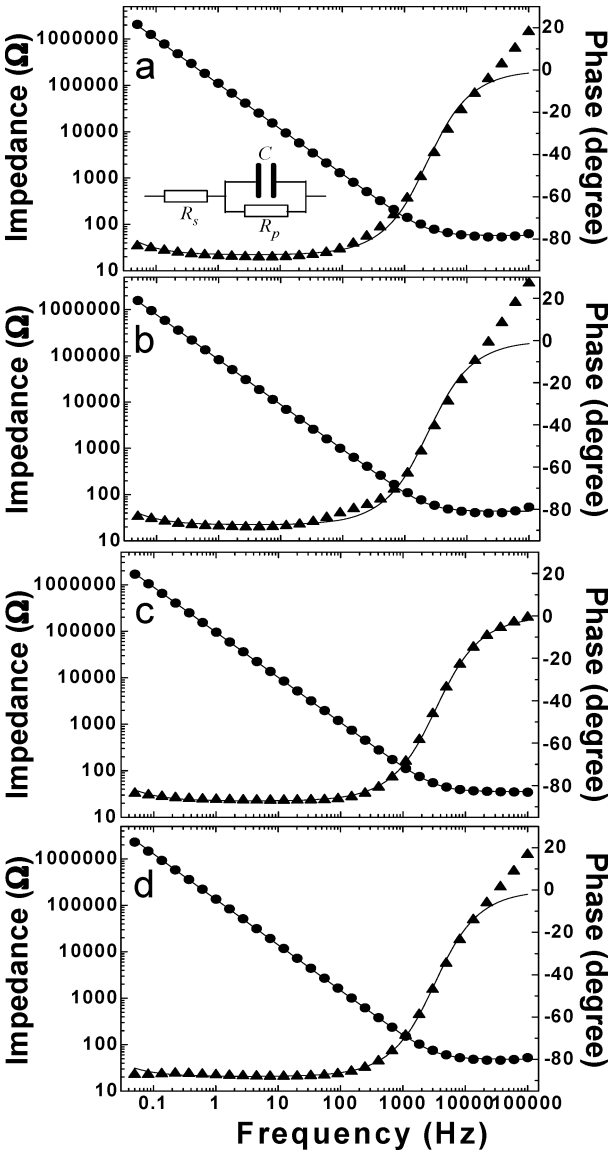

Figure 4. Electrochemical impedance spectra, i.e., the absolute impedance (circles) and phase shift (triangles) of the signal against frequency, of TPDMT/Au (a), CL-TPDMT/Au (b), Ni/TPDMT/Au (c), and Ni/CL-TPDMT/Au (d) in 0.1 M Na_2SO_4. The solid lines correspond to the fits performed within the equivalent circuit model which described in inset.

TABLE 1: Electrical Parameters of the TPDMT and CL-TPDMT Films Derived from the Impedance Spectroscopy Data within the Simplified Equivalent Circuit Model (See Text for Details)

	R_s (Ω)	C (μF cm^{-2})	R_p (MΩ cm^2)
pristine TPDMT	57.63	1.22	7.80
CL-TPDMT	43.52	1.58	15.2
Ni/pristine TPDMT	35.10	1.54	4.65
Ni/CL-TPDMT	48.14	1.11	13.6

conjugation between the individual phenyl rings along the terphenyl backbone of the TPDMT molecule upon the partial loss of hydrogen and subsequent cross-linking between the residual aromatic backbones.

At a careful examination of the phase shift curves for the pristine and cross-linked TPDMT SAMs, a small characteristic hump in the medium-frequency range from 100 to 1000 Hz was observed. To investigate the hump, we measured the potential dependence of the impedance spectra for the CL-TPDMT SAM. Figure 5 shows impedance spectra of this system at three

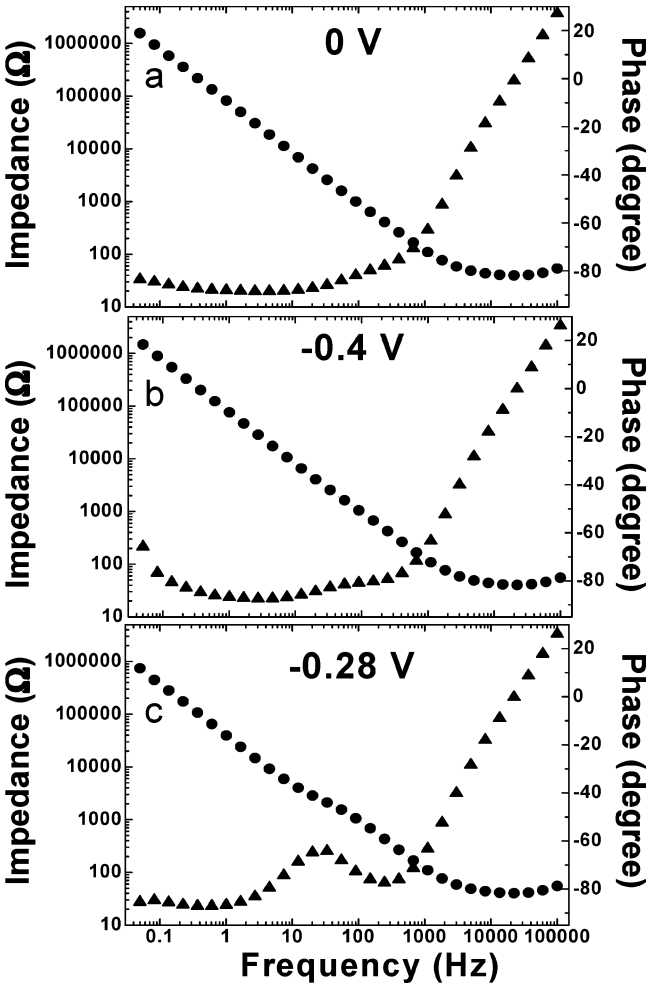

Figure 5. Impedance spectra for CL-TPDMT/Au in 0.1 M Na_2SO_4 acquired at electrode potentials of 0 (a), −0.4 (b), and −0.28 V (c).

different electrode potentials, *V*. While there is a small hump at $V = 0$ V (Figure 5a) and $V = -0.4$ V (Figure 5b), a relatively large hump is observed at $V = -0.28$ V (Figure 5c), at which the redox reaction occurs in the TPDMT and CL-TPDMT SAMs (see Figure 1b,c). Thus, the hump is presumably related to the redox-active sites in the interior of these films.

At the same time, no hump was observed in impedance spectra of Ni/TPDMT/Au and Ni/CL-TPDMT/Au, which looked very similar to previously reported impedance spectra of alkanethiol SAMs.[27] In accordance with the conclusion derived on the basis of the CV curves, these results imply that the Ni top layer fabricated on the TPDMT and CL-TPDMT substrates prevents the access of ions to the redox-active sites in the film interior. In other words, the electron-transfer reactions through the redox-active sites of the TPDMT and CL-TPDMT SAM are inhibited by the presence of the Ni overlayer. This result also suggests that this layer is quite stable in the electrolyte solution, in accordance with the previous conclusions.

4. Conclusion

Pristine and cross-linked TPDMT SAMs and Ni/TPDMT and Ni/CL-TPDMT arrangements on gold electrodes were characterized by electrochemical tools, including cyclic voltammetry and impedance spectroscopy. In all cases, TPDMT and CL-TPDMT films were found to be insulators, which effectively blocked the ionic permeation of electrolyte, preventing direct access of ions to the metal electrodes. For CL-TPDMT/Au, charge-transfer reaction of the $Fe(CN)_6^{3-}/Fe(CN)_6^{4-}$ redox complexes was also monitored. This reaction was found to be effectively blocked by the CL-TPDMT film.

Whereas the capacitance of the TPDMT film was only slightly affected by its cross-linking, this procedure resulted in a noticeable increase of the film resistance. Thus, CL-TPDMT is a better insulator than the pristine TPDMT film. Most important, the insulating properties of CL-TPDMT were not affected by the fabrication of the Ni overlayer—the resistance and capacitance of this film in the Ni/CL-TPDMT/Au sandwich were found to be quite close to the values measured for CL-TPDMT before the Ni evaporation. Thus, the top Ni layer is electrically isolated from the Au substrate, and no short circuits occur.

The top Ni layer was found to be relatively stable at the broad potential range in the electrolyte solutions. Despite a partial oxidation, this layer is still conductive at 5 monolayer thickness. At the same time, due to the CL-TPDMT insulation, it behaves differently in the electrolyte solution as compared to the bare Ni electrode. In particular, the characteristic dissolving reaction of Ni was not observed for the top Ni layer when only the underlying Au substrate was contacted by the working electrode.

Acknowledgment. We thank W. Eck (Universität Heidelberg) and A. Terfort (Universität Hamburg) for synthesis of the TPDMT and TPMT substances. H.N. acknowledges the fellowship of the Japan Society of the Promotion Science (JSPS). This work has been supported by the German BMBF (Grant 05KS4VHA/4), EU STREP "Nanocues", and Fond der Chemie.

References and Notes

(1) Ulman, A. *An Introduction to Ultrathin Organic Films: Langmuir−Blodgett to Self-Assembly*; Academic Press: New York, 1991.
(2) Ulman, A. *Chem. Rev.* **1996**, *96*, 1533.
(3) Fendler, J. H. *Chem. Mater.* **2001**, *13*, 3196.
(4) Halik, M.; Klauk, H.; Zschiescnang, U.; Schmid, G.; Dehm, C.; Schütz, M.; Maisch, S.; Effenberger, F.; Brunnbauer, M.; Stellacc, F. *Nature* **2004**, *431*, 963.
(5) Tsymball, E. Y.; Mryasov, O. N.; LeClair, P. R. *J. Phys. Condens. Matter* **2003**, *15*, R109.
(6) Meyerheim, H. L.; Popescu, R.; Kirschner, J.; Jedrecy, N.; Sauvage-Simkin, M.; Heinrich, B.; Pinchaux, R. *Phys. Rev. Lett.* **2001**, *87*, 076102-1.
(7) Park, S.; Keavney, D. J.; Falco, C. M. *J. Appl. Phys.* **2004**, *95*, 3037.
(8) Wold, D. J.; Haag, R.; Rampi, M. A.; Frisbie, C. D. *J. Phys. Chem. B* **2002**, *106*, 2813.
(9) Beebe, J. M.; Engelkes, V. B.; Miller, L. L.; Frisbie, C. D. *J. Am. Chem. Soc.* **2002**, *124*, 11268.
(10) Holmlin, R. E.; Haag, R.; Chabinyc, M. L.; Ismagilov, R. F.; Cohen, A. E.; Terfort, A.; Rampi, M. A.; Whitesides, G. M. *J. Am. Chem. Soc.* **2001**, *123*, 5075.
(11) Mann, B.; Kuhn, H. *J. Appl. Phys.* **1971**, *42*, 4398.
(12) Boulas, C.; Davidovits, J. V.; Rondelez, F.; Vuillaume, D. *Phys. Rev. Lett.* **1996**, *76*, 4749.
(13) Vuillaume, D.; Boulas, C.; Collet, J.; Davidovits, J. V.; Rondelez, F. *Appl. Phys. Lett.* **1996**, *69*, 1646.
(14) Rampi, M. A.; Schueller, O. J. A.; Whitesides, G. M. *Appl. Phys. Lett.* **1998**, *72*, 1781.
(15) Tai, Y.; Shaporenko, A.; Rong, H.-T.; Buck, M.; Eck, W.; Grunze, M.; Zharnikov, M. *J. Phys. Chem. B* **2004**, *108*, 16806.
(16) Zharnikov, M.; Frey, S.; Rong, H.-T.; Yang, Y. J.; Heister, K.; Buck, M.; Grunze, M. *Phys. Chem. Chem. Phys.* **2000**, *2*, 3359.
(17) Rong, H.-T.; Frey, S.; Yang, Y. J.; Zharnikov, M.; Buck, M.; Wühn, M.; Wöll, Ch.; Helmchen, G. *Langmuir* **2001**, *17*, 1582.
(18) Azzam, W.; Cyganik, P.; Witte, G.; Buck, M.; Wöll, Ch. *Langmuir* **2003**, *19*, 8262.
(19) Shaporenko, A.; Brunnbauer, M.; Terfort, A.; Grunze, M.; Zharnikov, M. *J. Phys. Chem. B* **2004**, *108*, 14462.
(20) Ishida, T.; Mizutani, W.; Akiba, U.; Umemura, K.; Inoue, A.; Choi, N.; Fujihira, M.; Tokumoto, H. *J. Phys. Chem. B* **1999**, *103*, 1686.
(21) Tai, Y.; Shaporenko, A.; Noda, H.; Grunze, M.; Zharnikov, M. *Adv. Mater.* **2005**, *17*, 1745.
(22) Tai, Y. Ph.D. Thesis, Universität Hiedelberg, Heidelberg, Germany, 2004.

(23) Gayer, W.; Stadler, V.; Eck, W.; Zharnikov, M.; Gölzhäuser, A.; Grunze, M. *Appl. Phys. Lett.* **1999**, *75*, 2401.
(24) Zharnikov, M.; Grunze, M. *J. Vac. Sci. Technol., B* **2002**, *20*, 1793.
(25) Adlkofer, K.; Shaporenko, A.; Zharnikov, M.; Grunze, M.; Ulman, A.; Tanaka, M. *J. Phys. Chem. B* **2003**, *107*, 11737.
(26) Sabatani, E.; Cohen-Boulakia, J.; Bruening, M.; Rubinstein, I. *Langmuir* **1993**, *9*, 2974.
(27) Boubour, E.; Lennox, R. B. *Langmuir* **2000**, *16*, 4222.
(28) Esplandiú, M. J.; Hagenström, H.; Kolb, D. M. *Langmuir* **2001**, *17*, 828.
(29) Tai, Y.; Shaporenko, A.; Eck, W.; Grunze, M.; Zharnikov, M. *Langmuir* **2004**, *20*, 7166.
(30) Bard, A. J.; Faulkner, L. R. *Electrochemical Methods: Fundamentals and Applications*; Wiley-Interscience: New York, 2000.